Tellus (1994), 46A, 566–582
Printed in Belgium – all rights reserved


TELLUS
ISSN 0280–6495

# The generation of available potential energy, according to Lorenz' exact and approximate equations

By PETER SIEGMUND, *Royal Netherlands Meteorological Institute, P.O. Box 201, 3730 AE De Bilt, The Netherlands*

(Manuscript received 13 August 1993; in final form 13 December 1993)

ABSTRACT

The generation of available potential energy (APE) in the atmosphere according to Lorenz' (1955a, b) exact and approximate equations is investigated in the space-time domain. The generation is determined from the fields of diabatic heating and temperature. The heating is evaluated by the residual method, using 4 × daily ECMWF-(European Centre for Medium-Range Weather Forecasts) initialised analyses for the January months of 1986–1992 and the July months of 1985–1991. The contributions of different parts of the atmosphere to the exact and approximate generation are investigated, and the differences between these contributions are explained. In the derivation of the equation of the approximate generation, Lorenz made several approximations. The most serious one appears to be that the average pressure on an isentropic surface is approximately equal to the pressure of the isobaric surface, for which the average potential temperature is equal to the potential temperature of the isentropic surface. Our results show that the largest differences between the contributions to the exact and approximate generation occur in the extratropical low troposphere. Here the contribution to the exact generation of eddy APE is up to 10 × smaller than in the approximation, and the contribution to the exact generation of zonal- and time-mean APE is weakly positive, whereas for the approximation it is strongly negative. Other main differences occur in the tropical middle troposphere where the contribution to the exact generation of mean APE is about two times as small as the approximate value. Despite these large differences, the globally averaged exact generation of mean APE, which is 2.29 W/m$^2$ in January and 1.88 W/m$^2$ in July, differs less than 3 % from its approximation. The globally averaged exact generation of stationary eddy APE, which is 0.26 W/m$^2$ in January and 0.45 W/m$^2$ in July, is about 25% smaller than its approximation. In most individual months the globally averaged exact generation of transient eddy APE is weakly positive (about 0.01 W/m$^2$), whereas the approximation is weakly negative (about $-0.08$ W/m$^2$). The globally averaged generation of mean APE is not sensitive to the period and kind of the circulation data. The sensitivity of the globally averaged generation of stationary and transient eddy APE is about 0.1 W/m$^2$.

## 1. Introduction

The generation of available potential energy (APE) is an important component of the atmospheric energy cycle, since it describes how the potential energy of the atmosphere, which is continuously converted to kinetic energy, is maintained by diabatic heating. Lorenz (1955a, b) derived the so-called "exact" and approximate equations for the generation of mean and eddy APE. The "exact" generation is determined by the product of diabatic heating and an efficiency factor, while the approximation is determined by the product of diabatic heating and temperature anomalies (see Section 2). Although the "exact" equations are based on several assumptions, we will hereafter omit the quotes of "exact". These assumptions are that (1) the atmosphere is in hydrostatic balance and (2) is stably stratified, (3) latent energy does not contribute to internal energy, and (4) surface topography can be ignored (see also Taylor, 1979).

The most recent study on the exact generation is probably the study of Newell et al. (1974). In this study, the attention is restricted to the generation of zonal- and time-mean APE. The exact generation has also been estimated by Dutton and Johnson (1967). Wiin-Nielsen and Brown (1962), Brown (1964), and Lawniczak (1970) estimated from diabatic heating and temperature observations the approximate generation of APE. In the period after 1974 the accuracy of atmospheric data has, especially for the heating, strongly been improved (see, e.g., Hoskins et al., 1989). In studies on the generation published after 1974 the attention, however, is restricted to the approximate generation (e.g., Oort and Peixoto, 1983; Arpe et al., 1986; Ulbrich and Speth, 1991). The accuracy of these recent approximate estimates is not known. Particularly the generation of eddy APE is poorly known. It depends on the variation in time and longitude of diabatic heating, which is difficult to estimate accurately. In the study of Oort and Peixoto (1983) this value is simply assumed, while Arpe et al. (1986) find that the sign of the estimated generation of eddy APE depends on the kind of circulation data used (e.g., first-guess or 12 h forecast data).

In the present paper the generation of APE will be computed from recent atmospheric data, using Lorenz' (1955a, b) exact as well as approximate equations. The differences between the exact and approximate results will be investigated and explained, and the contribution from different parts of the atmosphere to the global integrals of the exact and approximate generation will be examined. The generation is separated in a zonal- and time-mean part, a stationary eddy part and a transient eddy part. The diabatic heating is computed as a residual in the thermodynamic energy equation, using 4 × daily initialised analyses from the European Centre for Medium-Range Weather Forecasts (ECMWF) for the January months of 1986–1992 and the July months of 1985–1991.

It should be mentioned that the generation of APE is a global concept, so that only the generation integrated over the total mass of the atmosphere has a physical meaning. Nevertheless it makes sense to investigate the contributions from different parts of the atmosphere to the global integral, because only with such an investigation differences between the global integrals of the exact and approximate generation can be explained.

In Section 2, Lorenz' exact and approximate equations for the generation of APE are presented, the differences between the exact and approximate equations are interpreted, and the ECMWF circulation data are described. In Section 3, the results for the exact and approximate generation are shown and their differences are explained. The results are evaluated in Section 4.

## 2. Theory and data

### *2.1. Lorenz' equations for the generation of available potential energy*

Lorenz' (1955a, b) exact expression for the generation of APE per unit of area, $G^e(P)$, is:

$$G^e(P) = \frac{1}{4\pi R^2} \int Nq \, \mathrm{d}m, \tag{1}$$

where $R$ is the mean radius of the earth, $N$ is an efficiency factor, and $q$ is the diabatic heating per unit of mass. $N$ and $q$ depend on latitude, longitude, altitude and time. The integral is taken over the entire mass ($m$) of the atmosphere. The efficiency factor $N$ is equal to

$$N = 1 - (\tilde{p}(\theta)/p)^{\kappa}, \tag{2}$$

where $p$ is pressure, $\theta = T(p_0/p)^{\kappa}$ is potential temperature, $\tilde{p}(\theta)$ in any point in the atmosphere is the globally averaged value of $p$ on the isentropic ($\theta$ = constant) surface that passes through that point, $T$ is temperature, $p_0$ is a standard pressure of 1000 hPa, and $\kappa = (c_p - c_v)/c_p$, where $c_p$ and $c_v$ are the specific heats of dry air at constant pressure and volume, respectively. On those parts of the isentropic surface that are "below" the earth's surface, the pressure is set equal to the surface pressure. These parts can be regarded as coinciding with the earth's surface.

Because we want to explain differences between the exact and approximate generation, we will briefly repeat Lorenz' (1955b) derivation of the approximate expression. We will now describe this derivation as seven successive approximations, which will be numbered from I to VII. In approximation I, (2) is linearized:

$$N \approx \kappa \left( \frac{p - \tilde{p}(\theta)}{\tilde{p}(\theta)} \right). \tag{3}$$

Approximation II is that the average pressure on an isentropic surface is approximately equal to the pressure of the isobaric surface, for which the average potential temperature is equal to the potential temperature of the isentropic surface:

$$p \approx \tilde{p}(\tilde{\theta}(p)). \tag{4}$$

Although the tilde in (4) is used to denote averages over isentropic as well as isobaric surfaces, throughout this paper its meaning will always be clear, because the tilde will only be used for the symbols $\tilde{p}(\theta)$ and $\tilde{\theta}(p)$ (averages respectively over isentropic and isobaric surfaces). From (4) it follows that $p - \tilde{p}(\theta)$ can be approximated as

$$p - \tilde{p}(\theta) \approx \tilde{p}(\tilde{\theta}(p)) - \tilde{p}(\theta). \tag{5}$$

Next the right-hand side of (5) is approximated by the linear term of a Taylor-expansion (Approximation III):

$$\tilde{p}(\tilde{\theta}(p)) - \tilde{p}(\theta) \approx -\theta'' \, \partial\tilde{p}(\theta)/\partial\theta, \tag{6}$$

where $\theta'' \equiv \theta - \tilde{\theta}(p)$. It can be shown, by taking the partial derivative to $p$ of (4), that

$$\partial\tilde{p}(\theta)/\partial\theta \approx (\partial\tilde{\theta}(p)/\partial p)^{-1} \tag{7}$$

(approximation IV). Eq. (7) is exact if approximation II is exact. If $\tilde{\theta}(p)$ in (7) is approximated by its time average (approximation V), $\tilde{p}(\theta)$ in the dominator of (3) is approximated by $p$ (approximation VI), and $q$ in (1) is approximated by $q''$ (approximation VII), then successive substitution of (7), (6), (5), (3) and (1) gives Lorenz' (1955b) expression for the approximate generation:

$$G^{a}(P) = \frac{1}{4\pi R^2} \int \gamma_L T'' q'' \, \mathrm{d}m, \tag{8}$$

where the expression for the stability parameter $\gamma_L$ is

$$\gamma_L = -\left(\frac{\kappa}{p}\right)\left(\frac{\partial\{\bar{T}\}}{\partial p} - \kappa\frac{\{\bar{T}\}}{p}\right)^{-1}. \tag{9}$$

Assuming hydrostatic equilibrium, the time averages of (1) and (8) can be written as

$$\bar{G}^{e}(P) = G^{e}(P_M) + G^{e}(P_{SE}) + G^{e}(P_{TE}), \tag{10}$$

$$\bar{G}^{a}(P) = G^{a}(P_M) + G^{a}(P_{SE}) + G^{a}(P_{TE}), \tag{11}$$

where

$$G^{e}(P_M) = \frac{1}{2}\int_{-\pi/2}^{\pi/2}\int_0^{p_s} \frac{1}{g}[\bar{N}][\bar{q}] \times \cos(\phi)\, \mathrm{d}\phi\, \mathrm{d}p, \tag{10a}$$

$$G^{e}(P_{SE}) = \frac{1}{2}\int_{-\pi/2}^{\pi/2}\int_0^{p_s} \frac{1}{g}[\bar{N}^*\bar{q}^*] \times \cos(\phi)\, \mathrm{d}\phi\, \mathrm{d}p, \tag{10b}$$

$$G^{e}(P_{TE}) = \frac{1}{2}\int_{-\pi/2}^{\pi/2}\int_0^{p_s} \frac{1}{g}[\overline{N'q'}] \times \cos(\phi)\, \mathrm{d}\phi\, \mathrm{d}p, \tag{10c}$$

$$G^{a}(P_M) = \frac{1}{2}\int_{-\pi/2}^{\pi/2}\int_0^{p_s} \frac{\gamma_L}{g}[\bar{T}]''\,[\bar{q}]'' \times \cos(\phi)\, d\phi\, \mathrm{d}p, \tag{11a}$$

$$G^{a}(P_{SE}) = \frac{1}{2}\int_{-\pi/2}^{\pi/2}\int_0^{p_s} \frac{\gamma_L}{g}[\bar{T}^*\bar{q}^*] \times \cos(\phi)\, d\phi\, \mathrm{d}p, \tag{11b}$$

$$G^{a}(P_{TE}) = \frac{1}{2}\int_{-\pi/2}^{\pi/2}\int_0^{p_s} \frac{\gamma_L}{g}[\overline{T'q'}] \times \cos(\phi)\, d\phi\, \mathrm{d}p. \tag{11c}$$

Here $g$ is the acceleration due to gravity, $p_s$ is the zonal- and time-mean surface pressure, $\phi$ is latitude, $[x]$ is the zonal mean of $x$, $\bar{x}$ is the time mean of $x$ (in the present study the monthly mean) and $x'$ and $x^*$ are the deviations of $x$ from $\bar{x}$ and $[x]$ respectively. Eqs. (10a, b, c) and (11a, b, c) are Lorenz' exact and approximate equations of the generation of zonal- and time-mean, stationary eddy and transient eddy APE, respectively. The integrands in (10a, b, c) and (11a, b, c) are expressed in units of W m$^{-2}$ Pa$^{-1}$. In (10a, b, c) and (11a, b, c), and in the rest of this paper, the $G$-symbols all denote globally averaged quantities. Besides $\gamma_L$ (9), 2 other expressions for the stability parameter frequently occur in the literature:

$$\gamma_A = -\left(\frac{\kappa}{p}\right)\left(\frac{\partial[\bar{T}]}{\partial p} - \kappa\frac{[\bar{T}]}{p}\right)^{-1}, \tag{12a}$$

$$\gamma_0 = p^{-2\kappa}\frac{1}{p_0}\int_0^{p_0} p^{2\kappa}\gamma_L(p)\, \mathrm{d}p. \tag{12b}$$

$\gamma_A$ was, for example, applied by Arpe et al. (1986), and $\gamma_0$ by Oort (1964). We will investigate for which form of $\gamma$ the resemblance between the exact and the approximate generation is best.

*2.2. The accuracy of the approximations II and IV in the derivation of the approximate generation*

As will be shown in Section 3, the main differences between the exact and approximate generation can be understood from approximation II, $p \approx \tilde{p}(\tilde{\theta}(p))$, and the related approximation IV, $\partial\tilde{p}(\theta)/\partial\theta \approx (\partial\tilde{\theta}(p)/\partial p)^{-1}$. Below we will discuss the accuracy of these approximations. In addition we will argue that approximation II almost only affects the generation of mean APE, and that the generation of eddy APE is almost only affected by approximation IV.

*2.2.1. The accuracy of the approximation $p \approx \tilde{p}(\tilde{\theta}(p))$.* The accuracy of $p \approx \tilde{p}(\tilde{\theta}(p))$ is determined by the distribution of $\theta$, which zonal average is shown in Fig. 1 for January 1986. On a surface that is isentropic as well as isobaric the values of $p$ and $\tilde{p}(\tilde{\theta}(p))$ are the same. As follows from Fig. 1, in the upper troposphere and stratosphere the isentropes are nearly isobars. Therefore at these levels the values of $p$ and $\tilde{p}(\tilde{\theta}(p))$ are nearly the same. This is revealed by Table 1, which shows for January 1986 the values of $\tilde{\theta}(p)$, $\tilde{p}(\tilde{\theta}(p))$, $\partial\tilde{p}(\theta)/\partial\theta$ and $(\partial\tilde{\theta}(p)/\partial p)^{-1}$ at 100, 500 and 1000 hPa. The values of $\partial\tilde{p}(\theta)/\partial\theta$ and $(\partial\tilde{\theta}(p)/\partial p)^{-1}$ are computed for the points $(\tilde{\theta}(p), \tilde{p}(\tilde{\theta}(p))$ and $(\tilde{\theta}(p), p)$, respectively. The results for January 1986 do not significantly deviate from results for other months.

Table 1. *Values of $\tilde{\theta}(p)$, $\tilde{p}(\tilde{\theta}(p))$, $\partial\tilde{p}(\theta)/\partial\theta$ and $(\partial\tilde{\theta}(p)/\partial p)^{-1}$ at 100, 500 and 1000 hPa for January 1986*

| $p$ (hPa) | $\tilde{\theta}(p)$ (K) | $\tilde{p}(\tilde{\theta}(p))$ (hPa) | $\partial\tilde{p}(\theta)/\partial\theta$ (hPa/K) | $(\partial\tilde{\theta}(p)/\partial p)^{-1}$ (hPa/K) |
|---|---|---|---|---|
| 100 | 400 | 104 | −0.8 | −0.8 |
| 500 | 314 | 525 | −13.0 | −17.4 |
| 1000 | 286 | 894 | −7.1 | −22.6 |

In the middle troposphere, represented by 500 hPa in Table 1, $\tilde{p}(\tilde{\theta}(p))$ is larger than $p$. To understand this, we refer to the distribution of $\theta$ in Fig. 1, which has the characteristics that the pressure on the isentropes is higher in the tropics than in the extratropics, and that this pressure difference increases with decreasing altitude. At 500 hPa the value of $\tilde{\theta}(p)$ is 314 K. In the tropics (equatorward of 30°) the pressure on the 314 K isentrope is more than 500 hPa, whereas in the extratropics it is less than 500 hPa. Because in the tropics the "distance" to the 500 hPa isobar is larger than in the extratropics, the value of $\tilde{p}(314\text{ K})$ is larger than 500 hPa.

In the lower troposphere, represented by 1000 hPa in Table 1, $\tilde{p}(\tilde{\theta}(p))$ is smaller than $p$. The pressure on the $\tilde{\theta}(1000\text{ hPa}) = 286$ K isentrope is either equal to or less than the surface pressure. Therefore, because the surface pressure is generally

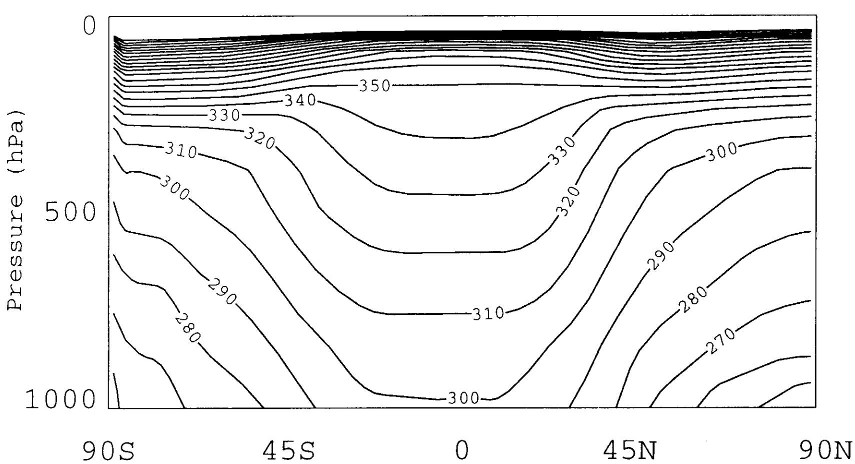


*Fig. 1.* Distribution of the zonal mean potential temperature, $[\bar{\theta}]$, in January 1986. Contour interval: 10 K.

less than 1000 hPa, the value of $\tilde{p}(\tilde{\theta}(1000\text{ hPa}))$ is less than 1000 hPa.

In (5) the approximation $p \approx \tilde{p}(\tilde{\theta}(p))$ is applied to estimate $p - \tilde{p}(\theta)$ in (3) by $\tilde{p}(\tilde{\theta}(p)) - \tilde{p}(\theta)$. In isobaric coordinates, the values of $p$ and $\tilde{p}(\tilde{\theta}(p))$ on a latitude circle do not vary with longitude. Therefore the stationary eddy parts of $p$ and $\tilde{p}(\tilde{\theta}(p))$ are zero. Consequently the stationary eddy parts of $p - \tilde{p}(\theta)$ and $\tilde{p}(\tilde{\theta}(p)) - \tilde{p}(\theta)$ are the same, so that the approximation $p \approx \tilde{p}(\tilde{\theta}(p))$ does not affect the generation of stationary eddy APE.

In isobaric coordinates also the transient part of $p$ is zero. The transient part of $\tilde{p}(\tilde{\theta}(p))$ is very small, because $\tilde{p}(\tilde{\theta}(p))$ only depends on global averages. Consequently the transient eddy parts of $\tilde{p} - \tilde{p}(\theta)$ and $\tilde{p}(\tilde{\theta}(p)) - \tilde{p}(\theta)$ are almost the same, so that the approximation $p \approx \tilde{p}(\tilde{\theta}(p))$ does hardly affect the generation of transient eddy APE.

The zonal- and time-mean parts of $p - \tilde{p}(\theta)$ and $\tilde{p}(\tilde{\theta}(p)) - \tilde{p}(\theta)$ are not necessarily the same. Therefore the approximation $p \approx \tilde{p}(\tilde{\theta}(p))$ might affect the generation of zonal- and time-mean APE.

*2.2.2. The accuracy of the approximation* $\partial\tilde{p}(\theta)/\partial\theta \approx (\partial\tilde{\theta}(p)/\partial p)^{-1}$. The accuracy of $\partial\tilde{p}(\theta)/\partial\theta \approx (\partial\tilde{\theta}(p)/\partial p)^{-1}$ follows from Fig. 2, which shows the functions $\tilde{\theta}(p)$ (solid curve) and $\tilde{p}(\theta)$ (dotted curve). The vertical distance between the two curves (defined positive if the solid curve is above the dotted curve) is equal to $\tilde{p}(\tilde{\theta}(p)) - p$. Therefore from Subsection 2.2.1 it follows that in the upper troposphere and stratosphere the two curves nearly coincide, whereas at 500 hPa the solid curve is slightly above and at 1000 hPa it is below the dotted curve. Because in the upper troposphere and stratosphere the two curves nearly coincide, here the values of $\partial\tilde{p}(\theta)/\partial\theta$ and $(\partial\tilde{\theta}(p)/\partial p)^{-1}$ are nearly the same, as shown in Table 1.

In the lower troposphere the value of $\partial\tilde{p}(\theta)/\partial\theta$, as revealed from Fig. 2, is very small. This is because for small values of $\theta$, which occur in the lower troposphere, a large part of the isentropic surfaces coincide with each other at the earth's surface. This effect is not seen in $(\partial\tilde{\theta}(p)/\partial p)^{-1}$, because it is determined by the average static stability on isobaric surfaces. Fig. 2 shows, however, that particularly for the small values of $\theta$ at high latitudes in the lower troposphere, the difference between $\partial\tilde{p}(\theta)/\partial\theta$ and $(\partial\tilde{\theta}(p)/\partial p)^{-1}$ is much larger than the difference that follows from Table 1. This is because, as mentioned above, the values of $\partial\tilde{p}(\theta)/\partial\theta$ in Table 1 are computed for $\theta = \tilde{\theta}(p)$, and therefore only apply for latitudes where $\theta = \tilde{\theta}(p)$. Fig. 1 shows that these latitudes are at about 30°. If $\theta$ approaches the lowest temperature found at the earth's surface, then the ratio $(\partial\tilde{\theta}(p)/\partial p)^{-1}/(\partial\tilde{p}(\theta)/\partial\theta)$ approaches infinity.

Fig. 2 shows also that in the middle troposphere the magnitude of $(\partial\tilde{\theta}(p)/\partial p)^{-1}$ is larger than the magnitude of $\partial\tilde{p}(\theta)/\partial\theta$, whereas in the upper troposphere the magnitude of $(\partial\tilde{\theta}(p)/\partial p)^{-1}$ is smaller than the magnitude of $\partial\tilde{p}(\theta)/\partial\theta$.

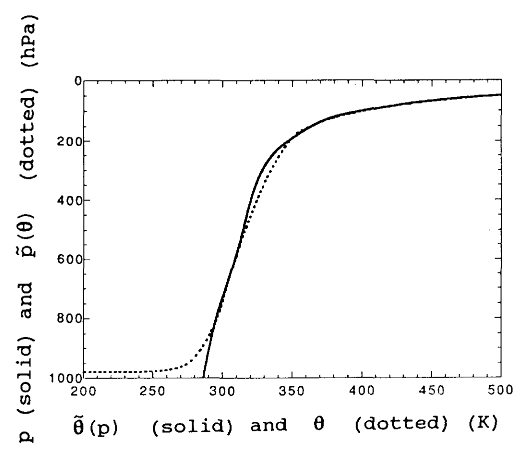


*Fig. 2.* Profiles of $\tilde{p}(\theta)$ (dotted) and $\tilde{\theta}(p)$ (solid), where $\tilde{p}(\theta)$ denotes pressure averaged over an isentropic surface, and $\tilde{\theta}(p)$ denotes potential temperature averaged over an isobaric surface.

### 2.3. *Data and method for calculating the diabatic heating*

The diabatic heating ($q$) is calculated as a residual in the thermodynamic energy equation for an ideal gas, which can be written as

$$q = c_{\mathrm{p}}\left(\frac{\partial T}{\partial t} + \frac{u}{R\cos(\phi)}\frac{\partial T}{\partial\lambda} + \frac{v}{R}\frac{\partial T}{\partial\phi} + \omega\left(\frac{\partial T}{\partial p} - \kappa\frac{T}{p}\right)\right), \qquad (13)$$

where $\lambda$ is longitude, $t$ is time, $u$ is zonal wind, $v$ is meridional wind and $\omega \equiv \mathrm{d}p/\mathrm{d}t$.

The circulation data that are applied in (13) ($u$, $v$, $\omega$ and $T$) are initialised analyses, obtained from the ECMWF, for the January months of 1986–1992 and July months of 1985–1991. We computed $q$ each day at 0, 6, 12 and 18 GMT, on 14 pressure levels (1000, 850, 700, 500, 400, 300, 250, 200, 150, 100, 70, 50, 30 and 10 hPa) for a global $2.5° \times 2.5°$ grid. More details about the computation of $q$ are given by Siegmund (1993).

## 3. Results

### *3.1. The generation of zonal- and time-mean available potential energy*

*3.1.1. The exact generation of mean APE* ($G^e(P_M)$). The exact generation of mean APE is determined by the zonal- and time-averages of the diabatic heating, $[\bar{q}]$, and the efficiency factor, $[\bar{N}]$ (see (10a)). We will firstly discuss the distribution of $[\bar{N}]$. The distributions of $[\bar{q}]$ for January 1986–1992 and July 1985–1991 are similar to the distributions for January 1986–1988 and July 1985–1987 that are shown and discussed by Siegmund (1993), and are therefore not considered in the present paper.

The January distribution of $[\bar{N}]$ is shown in Fig. 3. If the patterns of the two hemispheres are interchanged, the distribution becomes very similar to the July distribution, which is therefore not shown. In the lower troposphere $[\bar{N}]$ is positive everywhere. This is because in the reference state, which is the state with the lowest possible amount of total potential energy, and without available potential energy, the temperature in the lower troposphere is lower than in the actual state. As a result everywhere in the lower troposphere a diabatic heating (cooling) in the actual state will increase (decrease) the difference in temperature between the actual and the reference state, and will therefore increase (decrease) the amount of available potential energy. Thus in the lower troposphere a positive (negative) $q$ results in a positive (negative) contribution to $G^e(P_M)$, so that $N$ is positive in the lower troposphere. Both in January and July the largest positive values of $[\bar{N}]$ of around 0.10 occur in the stratosphere, at high latitudes of the summer hemisphere. The largest positive values in the troposphere are about 0.07, and occur in the tropics around 500 hPa. The largest negative values are in the upper troposphere at high latitudes of the winter hemisphere: less than $-0.28$ in January and less than $-0.35$ in July.

The local contributions in January and July to the exact generation of mean APE, $G^e(P_M)$, are shown in Figs. 4a and 5a, respectively. In most parts of the atmosphere the contribution to $G^e(P_M)$ is positive. The largest positive values (dense shading: more than $50 \times 10^{-6}$ W m$^{-2}$ Pa$^{-1}$) occur in the rising branch of the Hadley cell, where both $[\bar{N}]$ and $[\bar{q}]$ are positive, and at middle and high latitudes of the winter hemisphere, where both $[\bar{N}]$ and $[\bar{q}]$ are negative. The contribution to $G^e(P_M)$ is negative in the descending branch of the Hadley cell, where $[\bar{N}]$

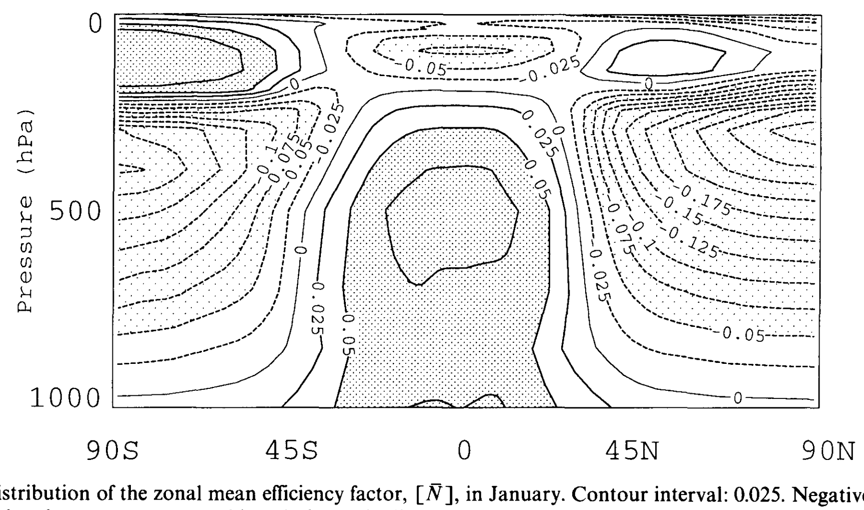


*Fig. 3.* Distribution of the zonal mean efficiency factor, $[\bar{N}]$, in January. Contour interval: 0.025. Negative contours are dashed and zero contours are thinned; dense shading: more than 0.05, light shading: less than $-0.05$.

is positive and $[\bar{q}]$ is negative, and in most of the stratosphere.

The value of $G^e(P_M)$ (i.e., the globally averaged exact generation of mean APE) is 2.29 W/m$^2$ in January and 1.88 W/m$^2$ in July. In the computation of global averages, the lower and middle troposphere near Antarctica (south of 60°S and below 500 hPa) is not included, because here the contribution to $G^e(P_M)$ shows unrealistic large positive and negative values. These values are due to errors in the diabatic heating, which in turn are due to errors in the circulation data. These errors are also found by Fortelius and Holopainen (1990) and Hoskins et al. (1989), and are probably due to the steep orography of Antarctica. The values of $G^e(P_M)$ for individual months are presented in Tables 2, 3. These values have an interannual variation of about 0.14 W/m$^2$, and do not show a specific trend.

*3.1.2. Differences between $G^e(P_M)$ and $G^a(P_M)$: description.* Figs. 4b and 5b show the local contributions to the approximate generation of mean APE, $G^a(P_M)$, in January and July, respectively. In the computation of $G^a(P_M)$ the stability parameter $\gamma_L$ (9) is applied. The main differences between the contributions to $G^a(P_M)$ and to $G^e(P_M)$ occur, as

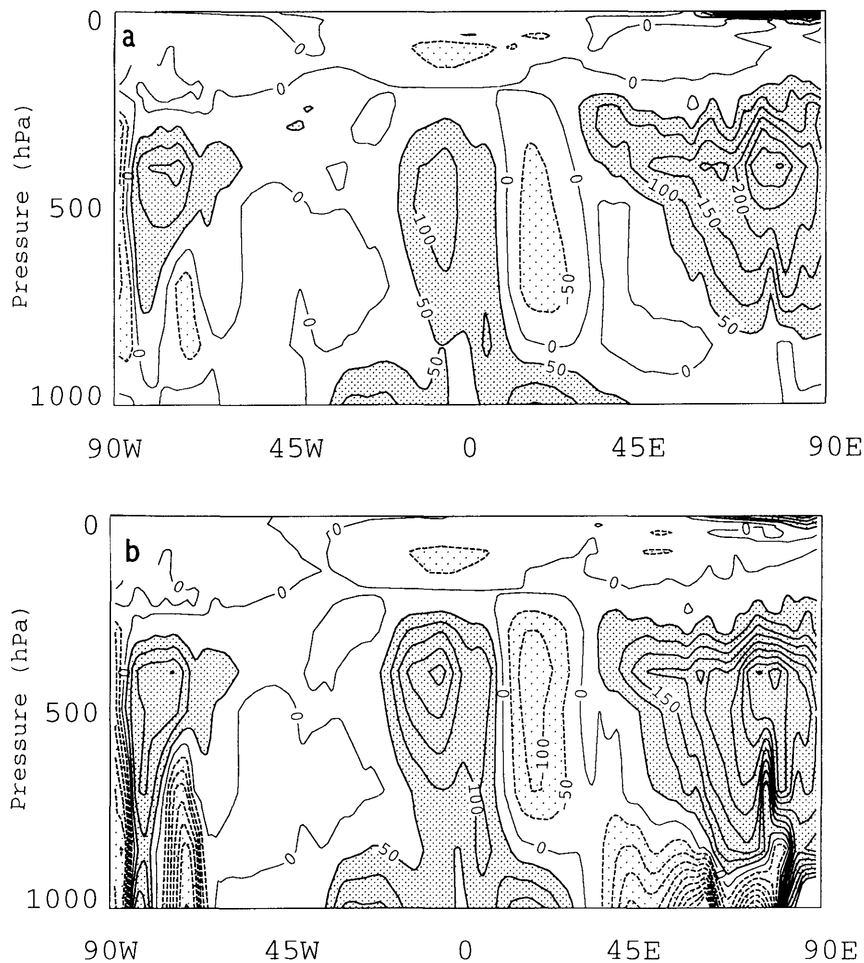


*Fig. 4.* Local contribution to the exact (a) and the approximate (b) generation of zonal- and time-mean available potential energy in January. Contour interval: $50 \times 10^{-6}$ W m$^{-2}$ Pa$^{-1}$; negative contours are dashed, zero contours are thinned. Dense shading: more than $50 \times 10^{-6}$ W m$^{-2}$ Pa$^{-1}$; light shading: less than $-50 \times 10^{-6}$ W m$^{-2}$ Pa$^{-1}$.

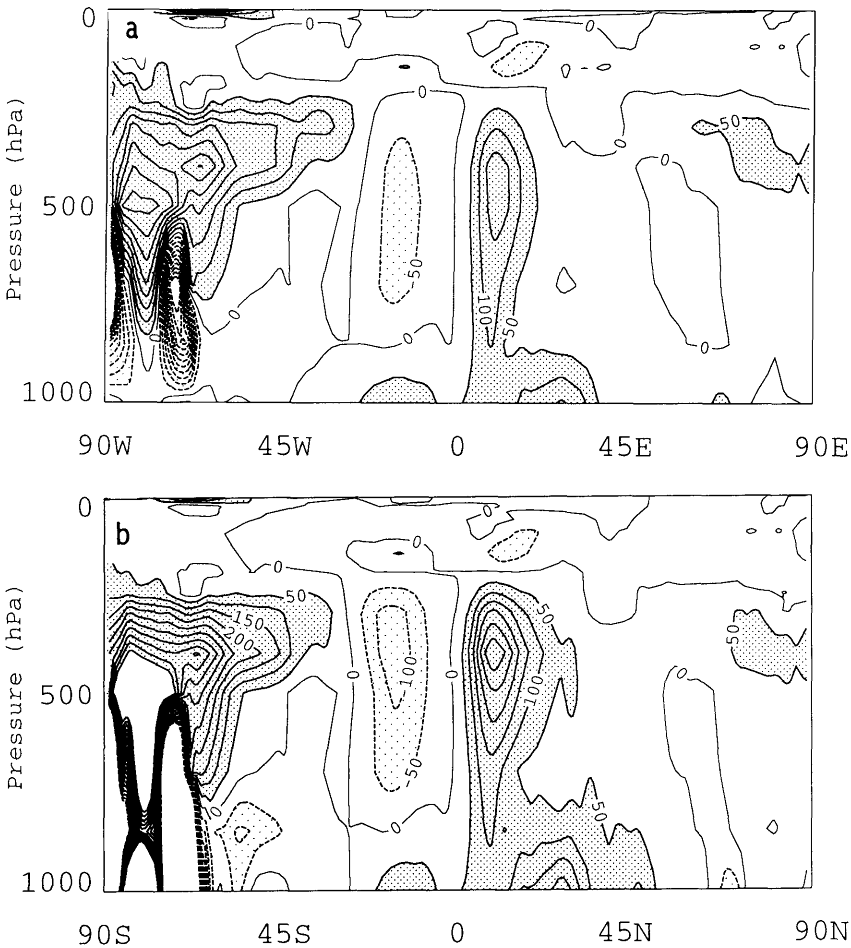


*Fig. 5.* As Fig. 4, but for July.

Table 2. *Globally averaged values for individual January months of the exact and approximate (indices e and a, respectively) generation of zonal- and time-mean, stationary eddy and transient eddy available potential energy ($P_M$, $P_{SE}$ and $P_{TE}$, respectively), and the average and standard deviation ($\sigma$) of these values ($W/m^2$)*

| | $G^e(P_M)$ | $G^a(P_M)$ | $G^e(P_{SE})$ | $G^a(P_{SE})$ | $G^e(P_{TE})$ | $G^a(P_{TE})$ |
|---|---|---|---|---|---|---|
| 1986 | 2.36 | 2.48 | 0.23 | 0.24 | 0.01 | −0.16 |
| 1987 | 2.22 | 2.29 | 0.24 | 0.29 | 0.06 | −0.10 |
| 1988 | 2.08 | 2.01 | 0.19 | 0.30 | −0.09 | −0.24 |
| 1989 | 2.20 | 2.15 | 0.25 | 0.32 | 0.03 | −0.14 |
| 1990 | 2.43 | 2.41 | 0.32 | 0.45 | −0.02 | 0.03 |
| 1991 | 2.48 | 2.60 | 0.30 | 0.46 | 0.04 | −0.14 |
| 1992 | 2.26 | 2.10 | 0.27 | 0.40 | 0.01 | 0.10 |
| average | 2.29 | 2.29 | 0.26 | 0.35 | 0.01 | −0.09 |
| $\sigma$ | 0.13 | 0.20 | 0.04 | 0.08 | 0.05 | 0.11 |

Table 3. *As Table 2, but for July*

| | $G^e(P_M)$ | $G^a(P_M)$ | $G^e(P_{SE})$ | $G^a(P_{SE})$ | $G^e(P_{TE})$ | $G^a(P_{TE})$ |
|---|---|---|---|---|---|---|
| 1985 | 1.65 | 1.61 | 0.29 | 0.35 | −0.09 | −0.17 |
| 1986 | 1.78 | 1.79 | 0.41 | 0.51 | 0.04 | −0.10 |
| 1987 | 2.05 | 2.02 | 0.41 | 0.49 | 0.06 | −0.06 |
| 1988 | 1.90 | 1.86 | 0.38 | 0.58 | 0.01 | −0.08 |
| 1989 | 2.11 | 2.07 | 0.58 | 0.71 | 0.05 | −0.00 |
| 1990 | 1.84 | 1.67 | 0.51 | 0.65 | −0.02 | −0.12 |
| 1991 | 1.83 | 1.79 | 0.57 | 0.71 | 0.04 | −0.02 |
| average | 1.88 | 1.83 | 0.45 | 0.57 | 0.01 | −0.08 |
| $\sigma$ | 0.15 | 0.16 | 0.11 | 0.12 | 0.05 | 0.05 |

already predicted by Dutton and Johnson (1967), in the lower troposphere in the extratropics of the northern hemisphere (NH) in January. Here the contribution to $G^a(P_M)$ is strongly negative, while the contribution to $G^e(P_M)$ is weakly positive. Other main differences occur in the tropical middle troposphere, where the contribution to $G^a(P_M)$ is much larger than the contribution to $G^e(P_M)$. The difference between the contributions to $G^a(P_M)$ and $G^e(P_M)$ is relatively small in the lower tropical troposphere, in the extratropical middle troposphere, and in the upper troposphere and stratosphere.

The value of $G^a(P_M)$ in January is 2.29 W/m$^2$, which is accidentally the same as the exact value (see Table 2). In July the value of $G^a(P_M)$ is 1.83 W/m$^2$, which is 3% less than the exact value. Also for individual months the difference between the exact and approximate global averages is small (less than 10%).

If the stability parameter $\gamma_0$ (12b) is used in stead of $\gamma_L$, then the values of $G^a(P_M)$ are about 25% smaller. These smaller global averages are due to a stronger negative contribution to $G^a(P_M)$ from the stratosphere, where $\gamma_0$ is much larger than $\gamma_L$. Experiments with $\gamma_A$ (12a) gave almost the same results as with $\gamma_L$. For most individual months, however, the best approximation was obtained with $\gamma_L$. Because $\gamma_L$ occurs in the derivation of the approximate generation and also gives the best approximation, $\gamma_L$ is used in the rest of this study.

*3.1.3. Differences between $G^e(P_M)$ and $G^a(P_M)$: explanation.* We will firstly discuss the effect of approximation II, $p \approx \tilde{p}(\tilde{\theta}(p))$, on the difference between $G^e(P_M)$ and $G^a(P_M)$ in the lower troposphere. As shown in Fig. 3 and explained in Subsection 3.1.1, in the lower troposphere the efficiency $N$ is positive everywhere. From the definition of $N$, (2), it follows that the signs of $N$ and $p - \tilde{p}(\theta)$ are the same, so that in the lower troposphere $p - \tilde{p}(\theta)$ is positive everywhere. As explained in Subsection 2.2.1, in the lower troposphere the approximation $\tilde{p}(\tilde{\theta}(p))$ of $p$ (approximation II) is smaller than $p$. Therefore in the lower troposphere the approximation $\tilde{p}(\tilde{\theta}(p)) - \tilde{p}(\theta)$ of $p - \tilde{p}(\theta)$ (see Subsection 2.2.1) is smaller than $p - \tilde{p}(\theta)$. The largest values of $N$ and $p - \tilde{p}(\theta)$ occur (see Fig. 3) at low latitudes. It appears that equatorward of about 30° $p - \tilde{p}(\theta)$ is larger and poleward $p - \tilde{p}(\theta)$ is smaller than $p - \tilde{p}(\tilde{\theta}(p))$. Therefore due to approximation II in the lower troposphere at low latitudes both $p - \tilde{p}(\theta)$ and $\tilde{p}(\tilde{\theta}(p)) - \tilde{p}(\theta)$ are positive but $\tilde{p}(\tilde{\theta}(p)) - \tilde{p}(\theta)$ is smaller than $p - \tilde{p}(\theta)$, whereas at high latitudes $p - \tilde{p}(\theta)$ is positive but $\tilde{p}(\tilde{\theta}(p)) - \tilde{p}(\theta)$ is negative. Consequently the effect of approximation II on the contribution to the generation in the lower troposphere is a decrease of this contribution from low latitudes, and a change of sign of this contribution from high latitudes. As explained in Subsection 2.2.1 this effect is restricted to the generation of mean APE.

In the lower troposphere, particularly at high latitudes, the magnitude of the approximation $(\partial\tilde{\theta}(p)/\partial p)^{-1}$ of $\partial\tilde{p}(\theta)/\partial\theta$ (approximation IV) is much larger than the magnitude of $\partial\tilde{p}(\theta)/\partial\theta$ (see Subsection 2.2.2). Therefore at low latitudes approximation II is partially cancelled by approximation IV, so that here the difference between the contributions to $G^e(P_M)$ and $G^a(P_M)$ is relatively small. At high latitudes, however, the negative contribution to $G^a(P_M)$ due to approximation II is strongly amplified by approximation IV.

In the middle troposphere between about 400 and 600 hPa the approximation $\tilde{p}(\tilde{\theta}(p))$ of $p$ (approximation II) is larger than $p$ (see Subsection 2.2.1). Therefore here the approximation $\tilde{p}(\tilde{\theta}(p)) - \tilde{p}(\theta)$ of $p - \tilde{p}(\theta)$ (see Subsection 2.2.1) is larger than $p - \tilde{p}(\theta)$. The sign of $p - \tilde{p}(\theta)$, which is the same as the sign of $N$, is positive at low latitudes. Therefore at low latitudes $\tilde{p}(\tilde{\theta}(p)) - \tilde{p}(\theta)$ is also positive, and is larger than $p - \tilde{p}(\theta)$. At high latitudes $p - \tilde{p}(\theta)$ is negative. At most high latitudes the difference between $p - \tilde{p}(\theta)$ and $\tilde{p}(\tilde{\theta}(p)) - \tilde{p}(\theta)$ appears to be small (i.e., smaller than $\tilde{p}(\tilde{\theta}(p)) - p$). Therefore at most high latitudes $\tilde{p}(\tilde{\theta}(p)) - \tilde{p}(\theta)$ is also negative, but less negative than $p - \tilde{p}(\theta)$.

Between about 400 and 600 hPa the magnitude of the approximation $(\partial\tilde{\theta}(p)/\partial p)^{-1}$ of $\partial\tilde{p}(\theta)/\partial\theta$ (approximation IV) is larger than the magnitude of $\partial\tilde{p}(\theta)/\partial\theta$ (see Subsection 2.2.2). Therefore at low latitudes approximation II is amplified by approximation IV, so that here the contribution to $G^{a}(P_{M})$ is much larger than the contribution to $G^{e}(P_{M})$. At high latitudes approximation II is partially cancelled by approximation IV, so that here the difference between the contributions to $G^{e}(P_{M})$ and $G^{a}(P_{M})$ is relatively small.

In the upper troposphere and stratosphere the approximations II and IV are accurate. Therefore here the difference between the contributions to $G^{e}(P_{M})$ and $G^{a}(P_{M})$ is small.

### 3.2. *The generation of stationary eddy available potential energy*

*3.2.1. The exact generation of stationary eddy APE ($G^{e}(P_{SE})$).* The zonally averaged contribution to $G^{e}(P_{SE})$ in January, shown in Fig. 6a, is dominated by positive patterns in the lower and upper troposphere. The positive contribution to $G^{e}(P_{SE})$ from the lower troposphere around 30° S is due to positive $\bar{N}^*$ and sensible heating (positive $\bar{q}^*$) over the summer continents (not shown). In the upper troposphere the contribution to $G^{e}(P_{SE})$ in the tropics is dominated by positive $\bar{N}^*$ and the release of latent heat (positive $\bar{q}^*$) over the eastern Pacific, whereas the positive contribution to $G^{e}(P_{SE})$ from midlatitudes is mainly due to negative $\bar{N}^*$ and radiative cooling (negative $\bar{q}^*$) over eastern Asia.

The zonally averaged contribution to $G^{e}(P_{SE})$ in July, shown in Fig. 7a, is dominated by positive patterns around 30° N in the lower and upper troposphere. In the lower troposphere the positive values are dominated by positive $\bar{N}^*$ and sensible heating (positive $\bar{q}^*$) over the Sahara and the Middle East (not shown). In the upper troposphere the positive values are mainly due to positive $\bar{N}^*$ and the release of latent heat (positive $\bar{q}^*$) in the monsoon region.

It follows from Figs. 6a and 7a that in most regions the contribution to $G^{e}(P_{SE})$ is positive. The value of $G^{e}(P_{SE})$ is 0.26 W/m$^2$ in January and 0.45 W/m$^2$ in July.

*3.2.2. Differences between $G^{e}(P_{SE})$ and $G^{a}(P_{SE})$.* The zonally averaged contribution to the approximate generation of stationary eddy APE, $G^{a}(P_{SE})$, is shown in Fig. 6b for January and in Fig. 7b for July. The largest differences between the contributions to $G^{a}(P_{SE})$ and $G^{e}(P_{SE})$ occur at low levels in the extratropics of the NH, where the contribution to $G^{a}(P_{SE})$ is much larger than the contribution to $G^{e}(P_{SE})$. Unlike the signs of the contributions to $G^{a}(P_{M})$ and $G^{e}(P_{M})$, the signs of the contributions to $G^{a}(P_{SE})$ and $G^{e}(P_{SE})$ are the same in this region. This is because the approximation II, which causes the different signs of the contributions to $G^{a}(P_{M})$ and $G^{e}(P_{M})$ from the extratropical lower troposphere (see Subsection 3.1.3), does not affect the generation of stationary eddy APE (see Subsection 2.2.1). The main differences between the contributions to $G^{a}(P_{SE})$ and $G^{e}(P_{SE})$ can be understood from approximation IV, $\partial\tilde{p}(\theta)/\partial\theta \approx (\partial\tilde{\theta}(p)/\partial p)^{-1}$, which in the lower troposphere amplifies the contribution to the generation, particularly at the high latitudes where $\theta$ is small (see Subsection 3.1.3). In the upper troposphere and stratosphere the differences between the contributions to $G^{a}(P_{SE})$ and $G^{e}(P_{SE})$ are small, because here the difference between $(\partial\tilde{\theta}(p)/\partial p)^{-1}$ and $\partial\tilde{p}(\theta)/\partial\theta$ is small.

Both in January and July the value of $G^{a}(P_{SE})$ is about 25% larger than the value of $G^{e}(P_{SE})$ (see Tables 2, 3).

### 3.3. *The generation of transient eddy available potential energy*

*3.3.1. The exact generation of transient eddy APE ($G^{e}(P_{TE})$).* The zonally averaged contributions to $G^{e}(P_{TE})$ in January and July, shown respectively in Figs. 8a and 9a, are dominated by positive patterns in the middle troposphere at midlatitudes. In the NH these patterns are mainly

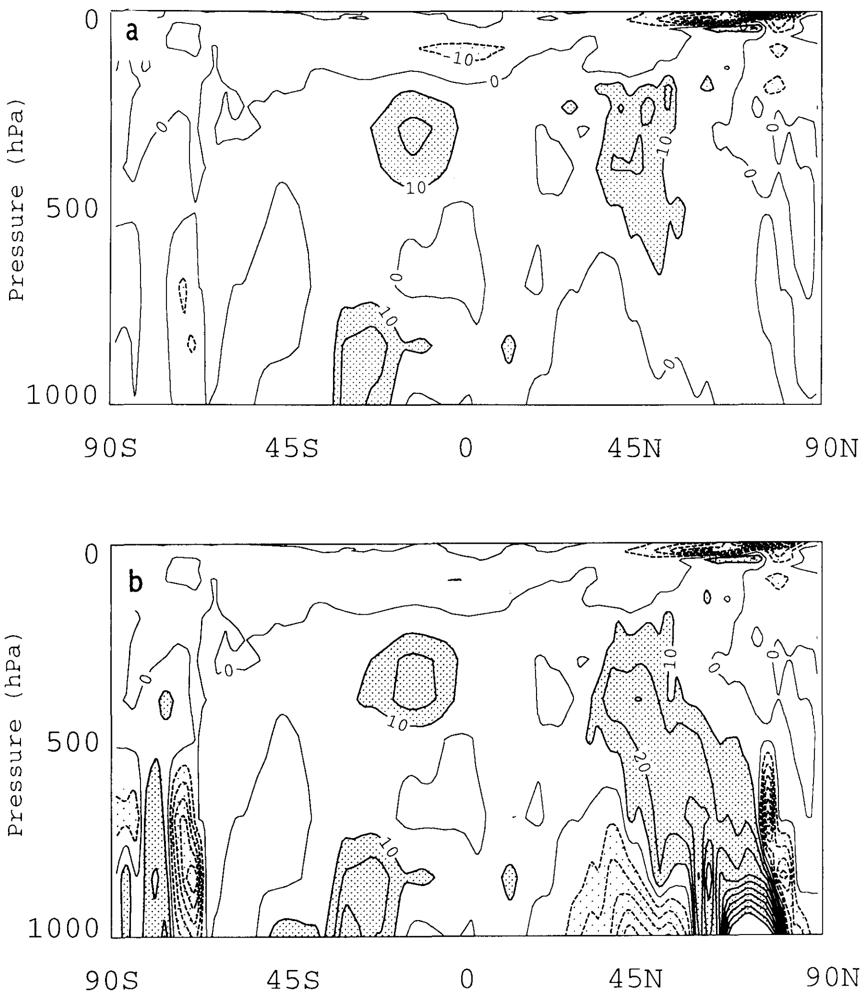


*Fig. 6.* Zonally averaged contribution to the exact (a) and the approximate (b) generation of stationary eddy available potential energy in January. Contour interval: $10 \times 10^{-6}$ W m$^{-2}$ Pa$^{-1}$; negative contours are dashed, zero contours are thinned. Dense shading: more than $10 \times 10^{-6}$ W m$^{-2}$ Pa$^{-1}$; light shading: less than $-10 \times 10^{-6}$ W m$^{-2}$ Pa$^{-1}$.

due to the positive contributions from the Atlantic and Pacific stormtracks (not shown). Negative zonally averaged contributions to $G^e(P_{TE})$, which are generally small, occur in most of the lower and upper troposphere, and in the stratosphere.

Globally averaged, the positive and negative values nearly cancel; the value of $G^e(P_{TE})$ is 0.01 W/m$^2$, both in January and July. For individual months its sign can be positive as well as negative (see Tables 2, 3).

*3.3.2. Differences between $G^e(P_{TE})$ and $G^a(P_{TE})$.* The zonally averaged contribution to the approximate generation of transient eddy APE, $G^a(P_{TE})$, is shown in Fig. 8b for January and in Fig. 9b for July. The largest differences between the contributions to $G^a(P_{TE})$ and $G^e(P_{TE})$ occur, as for the generation of stationary eddy APE, at low levels in the extratropics. Here the contribution to $G^a(P_{TE})$ is much stronger negative than the contribution to $G^e(P_{TE})$. As for the generation of stationary eddy APE, these differences can be understood from approximation IV, $\partial\tilde{p}(\theta)/\partial\theta \approx (\partial\tilde{\theta}(p)/\partial p)^{-1}$.

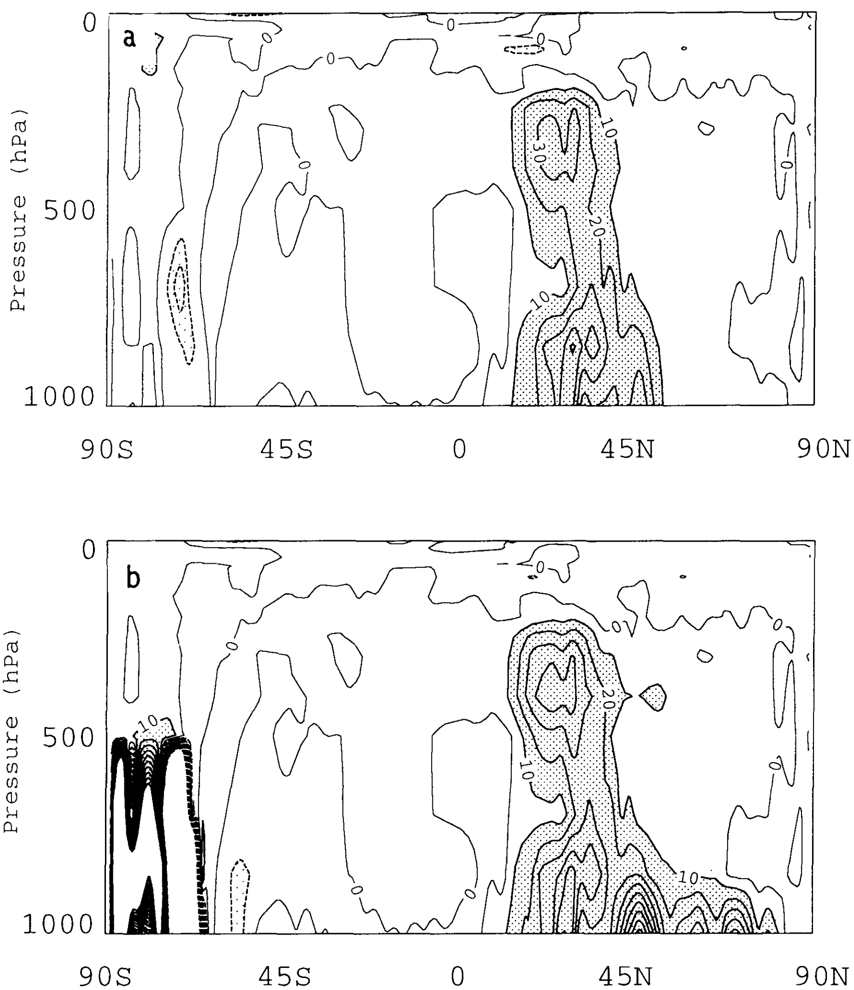


*Fig. 7.* As Fig. 6, but for July.

Other large differences occur at midlatitudes around 500 hPa, where the contribution to $G^a(P_{TE})$ is larger than the contribution to $G^e(P_{TE})$. A part of these differences is explained by approximation IV. The differences, however, also arise because at midlatitudes around 500 hPa the value of $p$ is smaller than the value of $\tilde{p}(\theta)$. Therefore in this region the contribution to the generation is also increased by the approximation of $\tilde{p}(\theta)$ in the denominator of (3) by $p$ (approximation VI in Subsection 2.1). The contribution to $G^a(P_{TE})$ from the extratropical middle troposphere is positive, because the release of latent heat, which in this region dominates the diabatic heating, is positively correlated with temperature. The contribution to $G^a(P_{TE})$ from the extratropical lower troposphere is negative, because the flux of sensible heat, which in this region dominates the diabatic heating, tends to smooth temperature variations. Both in January and July the estimated contribution to $G^a(P_{TE})$ agrees with the estimates of $[\overline{q'T'}]$ in the NH at 850 hPa by Saltzman (1973).

Both for the January and July ensemble average, the global average of $G^a(P_{TE})$ is, unlike the global average of $G^e(P_{TE})$, negative (see Tables 2, 3).

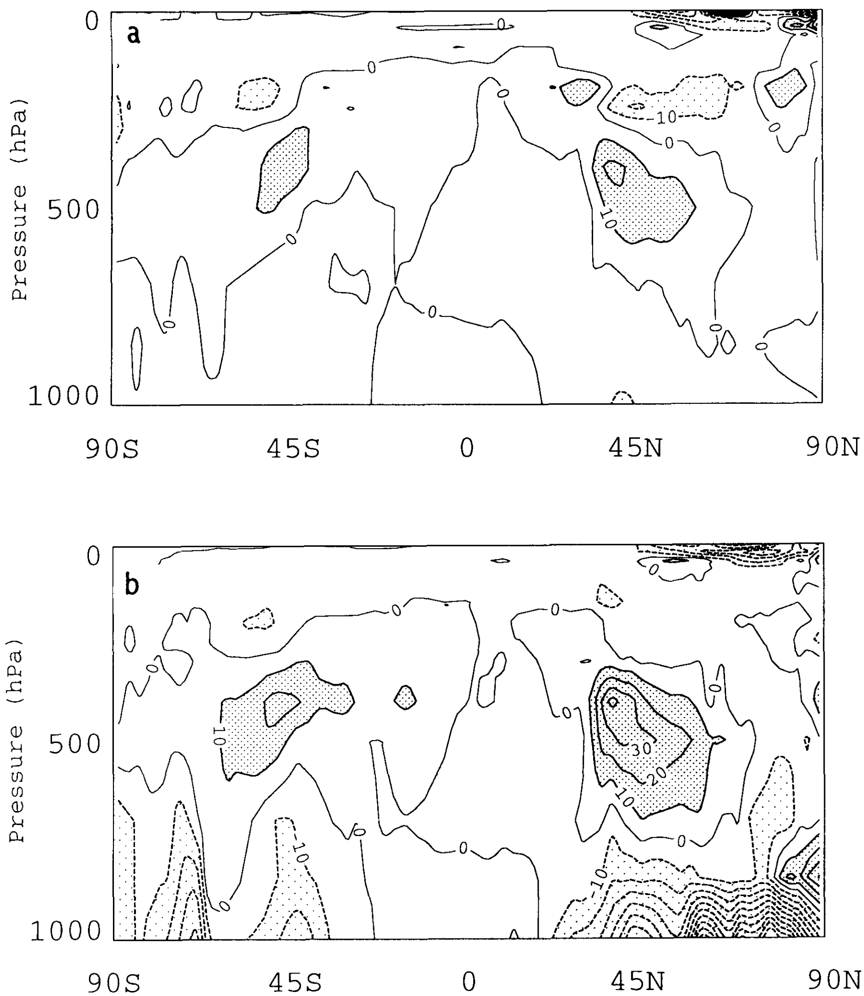


*Fig. 8.* Zonally averaged contribution to the exact (a) and the approximate (b) generation of transient eddy available potential energy in January. Contour interval: $10 \times 10^{-6}$ W m$^{-2}$ Pa$^{-1}$; negative contours are dashed, zero contours are thinned. Dense shading: more than $10 \times 10^{-6}$ W m$^{-2}$ Pa$^{-1}$; light shading: less than $-10 \times 10^{-6}$ W m$^{-2}$ Pa$^{-1}$.

### *3.4. Sensitivity of the results to kind and period of circulation data*

The error in the computed generation is mainly determined by the error in the computed residual heating. The residual heating depends on the kind of circulation data that is applied, e.g., initialised analyses or first-guess data. It also depends, particularly in the tropics (see Siegmund, 1993), on the parameterized heating in the model that provides the circulation data (in our case the ECMWF model). During the period of the circulation data used in this study the heating parameterization in the ECMWF model underwent several changes. We will now investigate the effect of these changes, and of the kind of circulation data that is applied, on the computed generation.

A particularly large revision of the heating parameterization in the ECMWF model was implemented in May 1989. This revision consists of a new radiation scheme, a new cumulus convec-

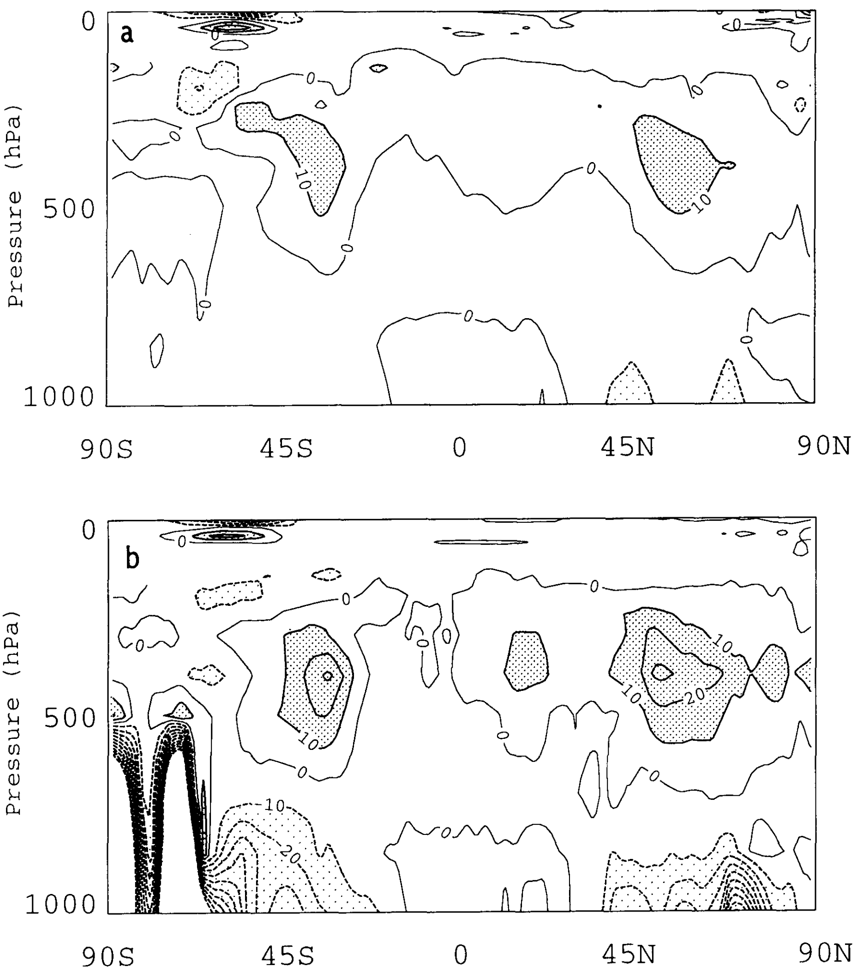


*Fig. 9.* As Fig. 8, but for July.

tion scheme, and a revised gravity wave drag (see, e.g., Hoskins et al., 1989). The main effects of these changes on the parameterized heating in the tropics (not shown) are more release of latent heat in the upward branch and more radiative cooling in the downward branch of the Hadley cell, and an increase of the longitudinal variability of the heating. Figs. 10a, b show the contributions to the exact generation of mean APE before (July 1988) and after (July 1989) the revision in May 1989. As expected, the largest differences occur in the tropics, where the contribution to the generation is much larger in July 1989 than in July 1988. The computed globally averaged generation of mean APE is hardly affected by the model changes (see Table 3), because of cancellation of positive and negative changes in local contributions. The computed globally averaged generation of stationary eddy APE, however, strongly increases after May 1989 (in the exact formulation from 0.19–0.25 $W/m^2$ before to 0.27–0.32 $W/m^2$ after May 1989 for January, and from 0.29–0.41 $W/m^2$ to 0.51–0.58 $W/m^2$ for July, see Tables 2 and 3). This is because the computed $\bar{q}^*$, which magnitude increases after May 1989, is positively correlated with $\bar{N}^*$. The computed globally averaged generation of transient eddy APE does not notably change after May 1989.

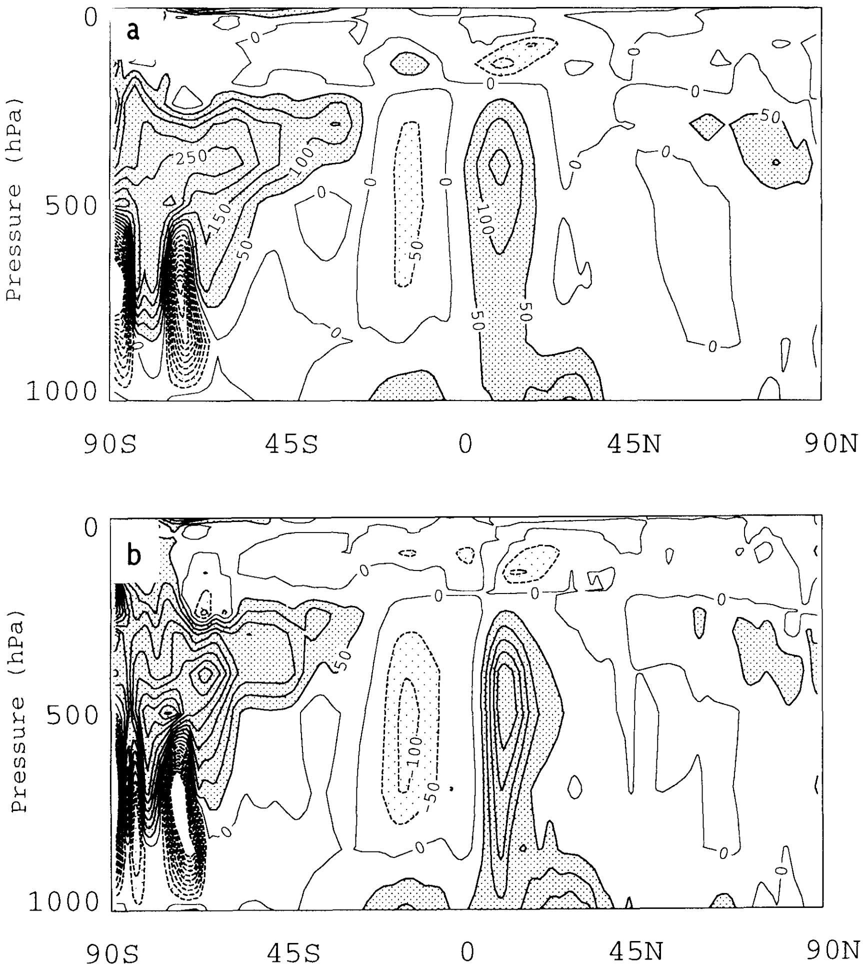


*Fig. 10.* Local contribution to the exact generation of zonal- and time-mean available potential energy before (a) and after (b) the changes in the ECMWF model in May 1989. (a): July 1988, (b): July 1989. Contour interval: $50 \times 10^{-6}$ W m$^{-2}$ Pa$^{-1}$; negative contours are dashed, zero contours are thinned. Dense shading: more than $50 \times 10^{-6}$ W m$^{-2}$ Pa$^{-1}$; light shading: less than $-50 \times 10^{-6}$ W m$^{-2}$ Pa$^{-1}$.

We investigated the sensitivity of the results to the kind of circulation data, by computing for one month (January 1990) the approximate generation from both initialised analyses and first-guess data. The values of $G^a(P_M)$, $G^a(P_{SE})$, and $G^a(P_{TE})$, computed from first-guess data, are 2.41, 0.47, and 0.14 W/m$^2$, respectively; the difference of these results with the values computed from initialised analyses (shown in Table 2) are 0.00, 0.02, and 0.11 W/m$^2$. Thus particularly the generation of transient eddy APE is sensitive to the kind of circulation data that is applied.

## 4. Conclusions

In this paper, the contributions from different parts of the atmosphere to the generation of available potential energy according to Lorenz' (1955a, b) exact and approximate equations are investigated in the space time domain. The main differences between the local contributions to the exact and approximate generation are explained. The generation is determined from the fields of diabatic heating and temperature. The diabatic heating is computed as a residual in the thermodynamic energy equation, using initialised analyses from ECMWF for the January months of 1986–1992 and the July months of 1985–1992.

For several parts of the atmosphere the difference between the contributions to the exact and approximate generation is large. The largest differences occur in the extratropics near the surface. We have shown that the main differences between the exact and approximate generation are due to the approximation $p \approx \tilde{p}(\tilde{\theta}(p))$ and the related approximation $\partial\tilde{p}(\theta)/\partial\theta \approx (\partial\tilde{\theta}(p)/\partial p)^{-1}$ (see Subsection 2.1) that were used by Lorenz (1955b) in his derivatation of the equations for the approximate available potential energy and its generation.

Despite these large differences between the local contributions to the exact and approximate generation, the difference between the globally averaged exact and approximate generation of total (zonal- and time-mean plus stationary and transient eddy) APE is very small (less than 1%). This small difference is due to cancellation of positive and negative differences between the local contributions to the exact and approximate generation. The differences for the globally averaged generation of mean APE are about 2%. The globally averaged exact and approximate generation of stationary eddy APE are positive, both in January and July, and differ about 25%. The globally averaged exact generation of transient eddy APE is positive, both in January and July, while the approximate values are negative. The difference between these exact and approximate values is about 0.10 W/m$^2$.

The estimated globally averaged generation of mean APE does not notably depend on the period of the circulation data nor on the kind of circulation data, and is therefore a good estimate of the real value. The corresponding stationary eddy estimate is about 0.1 W/m$^2$ larger after May 1989 than before, and the corresponding transient eddy estimate varies about 0.1 W/m$^2$ for different kinds of circulation data.

## 5. Acknowledgements

I wish to thank Reindert Haarsma, Cor Schuurmans, and two anonymous reviewers for critically reading the manuscript, and Abraham Oort for stimulating discussions. This work was supported by the Working Group on $CO_2$ Problems with financial aid from the Netherlands Organisation for Scientific Research (NWO).

## REFERENCES

Arpe, K., Brankovic, C., Oriol, E. and Speth, P. 1986. Variability in time and space of energetics from a long series of atmospheric data produced by ECMWF. *Beitr. Phys. Atmos.* **59**, 321–355.

Brown, J. A. 1964. A diagnostic study of tropospheric diabatic heating and the generation of available potential energy. *Tellus* **16**, 371–388.

Dutton, J. A. and Johnson, D. R. 1967. The theory of available potential energy and a variational approach to atmospheric energetics. *Adv. in Geophys.* **12** (Academic Press), pp. 333–436.

Fortelius, C. and Holopainen, E. O. 1990. Comparison of energy source estimates derived from atmospheric circulation data with satellite measurements of net radiation. *J. Climate* **3**, 646–660.

Hoskins, B. J., Hsu, H. H., James, I. N., Masutani, M., Sardeshmukh, P. D. and White, G. H. 1989. *Diagnostics of the global atmospheric circulation based on ECMWF analyses 1979–1989.* UGAMP Tech. Rep., No. 7. (Available from: Department of Meteorology, University of Reading, UK.)

Lawniczak, G. E. 1970. *Additional results from multilayer calculations of atmospheric diabatic processes and the generation of available potential energy.* Tech. Rep., No. 00263-2-T, University of Michigan, 71 pp.

Lorenz, E. N. 1955a. Generation of available potential energy and the intensity of the general circulation. In: *Large Scale Synoptic Processes* (J. Bjerknes, Proj. Director), Dept. Meteorol., Final Report, 1957, No. AF19(604)-1286. Univ. of California, Los Angeles, California.

Lorenz, E. N. 1955b. Available potential energy and the maintenance of the general circulation. *Tellus* **7**, 157–167.

Newell, R. E., Kidson, J. W., Vincent, D. G. and Boer, G. J. 1974. *The general circulation of the tropical atmosphere*, vol. 2, ch. 8, MIT press.

Oort, A. H. 1964. On estimates of the atmospheric energy cycle. *Mon. Wea. Rev.* **92**, 483–493.

Oort, A. H. and Peixoto, J. P. 1983. Global angular momentum and energy balance requirements from observations. *Adv. in Geophys.* **25**, 355–490.

Siegmund, P. C. 1993. Cloud diabatic forcing of the atmosphere, estimated from simultaneous ECMWF-diabatic heating and ISCCP-cloud amount observations. *J. Climate* **6**, 2419–2433.

Saltzman, B. 1973. Parameterization of hemispheric heating and temperature variance fields in the lower troposphere. *Pure Appl. Geophys.* **105**, 890–899.

Taylor, K. E. 1979. Formulas for calculating available potential energy over uneven topography. *Tellus* **31**, 236–245.

Ulbrich, U. and Speth, P. 1991. The global energy cycle of stationary and transient atmospheric waves: results from ECMWF analyses. *Meteorol. Atmos. Phys.* **45**, 125–138.

Wiin-Nielsen, A. and Brown, J. A. 1962. On diagnostic computations of atmospheric heat sources and sinks and the generation of available potential energy. *Proceedings of the International Symposium on Numerical weather prediction*, 7–13 November 1960, Tokyo, Meteorological Society of Japan, 593–613.